Optimal Harvesting Patterns for a Seaweed Harvester

Marco Gallieri[†] **and John Ringwood**[*]

[†] *Dipartimento di Ingegneria Informatica, Gestionale e dell'Automazione, UNIVPM, Ancona, Italy*

E-mail: gallieri.marco@gmail.com

[*] *Department of Electronic Engineering, NUI, Maynooth, Co. Kildare, Ireland*

E-mail: john.ringwood@eeng.nuim.ie

Abstract — **In this paper, a 9 degree of freedom seaweed harvester dynamical model is presented. The model presented describes the coupled dynamics of a vessel and a harvesting device, lifted by a winch, subject to sea waves disturbances. In order to find an appropriate harvesting path, which minimizes the harvester motions, the model response is simulated for different encounter angles. This 9 DOF seaweed harvester model is defined by merging the unified ship model, given in Fossen [1], Perez [2] , including the seakeeping fluid memory effects, and the Nielsen [3], Fard [4] 9 DOF ship-crane model, which includes an elastic coupling between the vessel and the harvester, and computes the harvester hydrodynamics, as in [5]. For the ship-harvester elastic coupling, a linear stiffness matrix, based on Shashikala *et al* [6], has been computed. The model obtained also includes the effects of the vessel forward speed, the wave and current loads, the ship propellers and motion control forces, and the winch motor dynamics. The motor dynamic is based on the control-oriented models of Messineo *et al* [7]. A mathematical formulation is first presented, and its assumptions are discussed. Then, a model simulation, obtained by modifying the Fossen *et al* [8] Simulink MSS Toolbox, and its results, are discussed. The harvester position variance and the RMSE index are compared, for the simulation results of different harvesting paths, and a compromise solution is discussed.**

Keywords — **Seaweed harvester, marine systems, offshore lifts, MSS Toolbox, multibody systems.**

I The Harvester Altitude Control Problem

The system to represent, shown in Figure 2, consists of a winch, located on a small ship, which is subject to ocean wave disturbances, and moves at an average constant speed, with a periodical turning manoeuvre, in low depth water. The winch lifts a harvester, suspended by a rope, which is subjected to the wave induced ship motion and the water environment interactions. A typical harvesting path follows a zig-zag shaped trajectory, as shown in Figure 1. The pattern orientation, $\bar{\chi}$, also called *encounter angle*, corresponds to the relative orientation between the longest straight line of the zig-zag path, and the wave mean direction. The goal of the control action is to obtain a desired constant harvester altitude, with respect of the seabed profile, taking into account the waves

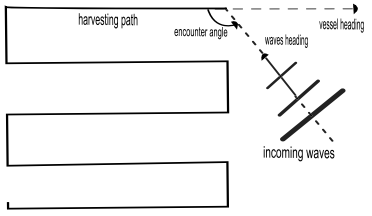

Fig. 1: *Relative pattern orientation* $\bar{\chi}$ definition

induced vessel and harvester motions, the winch dynamics and the rope stiffness. The control design is beyond the scope of this paper, while, the model presented here, will serve to examine the relationship between the encounter angle, and the magnitude of the wave induced disturbance, on the cutter altitude. In this paper, the optimal prob-

lem solution corresponds to a set of encounter angles, which reduce the disturbance variance and the RMSE, under a given threshold, to keep benefits on both the control design and performances.

II Reference Frames

A ship in a seaway moves in six degrees of freedom (6 DOF). The coordinates of motions are referred to *inertial frames* and *body-fixed frames*. The harvester moves also in 6 DOF, but for a control oriented model, only the 3 controllable translational DOF need to be considered, as in Fard [4]. The ship and harvester model presented here will have therefore 9 DOF. The 9 DOF model coordinate systems are shown in Figure 2.

For *marine systems*, the following right-hand frames are here considered, as in [2]:

- North-east-down frame (n-frame).

  The frame, (o_n, x_n, y_n, z_n), is used to define the absolute position of the vessel. The x-axis points towards the north, the y-axis towards the east, and the z-axis towards the center of the Earth.

- Ship body-fixed frame (b-frame).

  The frame, (o_b, x_b, y_b, z_b), fixed to the hull, is used to formulate the equations of motion. For marine vehicles, the axes are chosen to coincide with the principal axes of inertia, as shown in [2]. This determines the position of the origin of the frame, see [1] for details.

- Hydrodynamic ship frame (hs-frame).

  The frame, $(o_{hs}, x_{hs}, y_{hs}, z_{hs})$, is not fixed to the hull. It moves with the constant *average speed* of the vessel, following its path.

  The wave-induced forces make the vessel oscillate, with respect to the hs-frame, and are computed in this reference frame, is considered to be inertial. The positive x-axis points forward, and is aligned with the low frequency yaw angle, $\bar{\psi}$. The *"slowly-varying oscillations"* yaw angle, $\bar{\psi}$, is obtained by filtering out the first-order wave induced motion. Note that, $\bar{\psi}$ is constant, for a ship sailing in a straight line path, like a seaweed harvester. The frame origin is determined such that the z-axis passes through the *time-averaged position* of the vessel center of gravity.

For the *harvester motion*, the following right-hand frames are here considered:

- Hydrodynamic payload frame (hp-frame).

  The frame, $(o_{hp}, x_{hp}, y_{hp}, z_{hp})$, is not fixed to the harvester, and it's used to compute the force due to interactions between the harvester and the waves. As the hs-frame, the hp-frame moves at the *average speed* of the vessel, following its path. It is also subject to vertical motion, due to the altitude control actions, which are assumed are slowly varying, with respect to the harvester motions. The wave-induced forces are calculated in this reference frame, which is considered to be inertial. The frame origin is determined such that the z-axis passes through the *time-averaged position* of the harvester center of gravity.

- Winch frame (W-frame)

  The W-frame is not fixed to the hull, and its origin (o_w, x_w, y_w, z_w) coincides with the center of the winch motor axes. The frame is used for computing the winch motor equations.

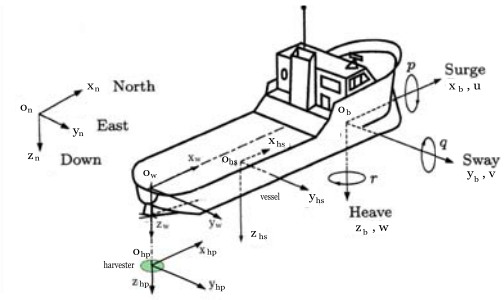

Fig. 2: *Reference frames*

III Kinematics of Ship and Harvester Motions

The equations of motion of the ship and the harvester are expressed in the b-frame. The wave forces are expressed in the hydrodynamic frames hs and hp. Some kinematic transformations are required to map the hs and the hp frames into the b-frame. For 6 DOF, the transformation between the hs-frame and the b-frame is given in Fossen [1] and Perez [2], as:

$$J_b^{hs}(\Theta_{hs-b}, r^b_{\bar{o}hs}) = \hat{J}_b^{hs}(\Theta_{hs-b}) H(r^b_{\bar{o}hs}) \tag{1}$$

where,

$$\hat{J}_b^{hs}(\Theta_{hs-b}) = \begin{bmatrix} R_b^{hs}(\Theta_{hs-b}) & 0_{(3\times3)} \\ 0_{(3\times3)} & T_\Theta(\Theta_{hs-b}) \end{bmatrix} \tag{2}$$

and

$$H(r^b_{\bar{o}hs}) = \begin{bmatrix} I_{(3\times3)} & S^T(r^b_{\bar{o}hs}) \\ 0_{(3\times3)} & I_{(3\times3)} \end{bmatrix} \tag{3}$$

In equation (2) the R_b^{hs} is the Euler angle rotation matrix, and T_Θ is the angular velocity transformation matrix, given in [2],[1]. Θ_{hs-b} is the Euler angle vector between the hs- and b-frame, In equation (3), $S(\lambda)$ is a skrew symmetric matrix, used for the cross product, and $r^b_{\bar{o}hs}$ is the vector

of the equilibrium position of the hs-frame origin, expressed in the b-frame. See Perez [2], and Fossen [1] more details about the above coefficients. Assuming small angles, $\Theta_{hs-b} \approx 0$, and a slender ship [9], the following approximations are taken:

$$\hat{J}_b^{hs}(\Theta_{hs-b}) \approx I_{(6\times 6)} \ , \tag{4}$$

such that ,

$$J_b^{hs}(\Theta_{hs-b}, r^b_{\bar{o}hs}) \approx J_b^{hs}(r^b_{\bar{o}hs}) = H(r^b_{\bar{o}hs}). \tag{5}$$

A similar approach can be taken for 9 DOF. First, the case of zero forward speed is described. The vector r^b_{ohp}, the origin the hp-frame in the b-frame reference, points from the b-frame origin o_b to the time averaged position of the center of the payload o_{hp}, when the spring is at rest. r^b_{ohp} is subject to 2-dimensional pendulum motion, given by:

$$r^b_{ohp} = R_b^{hp}(\Theta^b_{hp-b}) r^b_{\bar{o}hp} \tag{6}$$

where the Euler angle vector between the hp and the b-frame is $\Theta^b_{hp-b} \approx \begin{bmatrix} \phi^b & \theta^b & 0 \end{bmatrix}^T$.

In equation (6), $r^b_{\bar{o}hp}$ is the vector of the equilibrium position of the hp-frame origin, expressed in the b-frame. At this stage, for the b- to hp-frame transformation, the small angle approximation,

$$R_b^{hp}(\Theta^b_{hp-b}) \approx I_{(3\times 3)} \tag{7}$$

is taken, instead of the more accurate eq.(8),

$$R_b^{hp}(\Theta^b_{hs-b}) \approx I_{(3\times 3)} + S(\Theta^b_{hp-b}), \tag{8}$$

such that the b to hp-frame transformation is linear, and has the same form as eq.(3), and the couplings in the b-frame equation of motion are linear.

The *9 DOF body fixed to hydrodynamic frames transformation* is assumed to be:

$$J_b^h(r^b_{\bar{o}hs}, r^b_{\bar{o}hp}) \approx H(r^b_{\bar{o}hs}, r^b_{\bar{o}hp}),$$

$$H(r^b_{\bar{o}hs}, r^b_{\bar{o}hp}) = \begin{bmatrix} I_{(3\times 3)} & S^T(r^b_{\bar{o}hs}) & 0_{(3\times 3)} \\ 0_{(3\times 3)} & I_{(3\times 3)} & 0_{(3\times 3)} \\ 0_{(3\times 3)} & S^T(r^b_{\bar{o}hp}) & I_{(3\times 3)} \end{bmatrix} \tag{9}$$

The $r^b_{\bar{o}hp}$ vector is a function of the slowly varying motor position component $\bar{z}^W_m$, expressed in the W-frame, so the transformation given in eq.(9) is time varying. The slow varying component $\bar{z}^W_m$ is assumed, such that $\dot{r}^b_{\bar{o}hp} \approx 0$ and $\dot{J}^h_b \approx 0$. The generalized perturbation velocity, for zero forward speed, expressed in the h space, can be approximated by:

$$\dot{\boldsymbol{\xi}} = J_b^h(r^b_{\bar{o}hs}, r^b_{\bar{o}hp})\boldsymbol{\nu} \tag{10}$$

where the matrix $J_b^h(r^b_{\bar{o}hs}, r^b_{\bar{o}hp})$ is linear.

In the case of a forward speed, U, it's assumed that $\boldsymbol{\nu} = \bar{\nu} + \delta\boldsymbol{\nu}$, where $\delta\boldsymbol{\nu}$ is the b-frame velocity perturbation vector, and $\bar{\nu}$ is the slowly-varying b-frame velocity vector, given by, for 6 DOF [10]:

$$\bar{\nu}_6 = \begin{bmatrix} \bar{\nu_3}^T & 0_{(3\times 3)} \end{bmatrix}, \quad \bar{\nu_3} = U \ col_1\{(R_b^{hs})^T\} \ , \tag{11}$$

where $col_1\{R\}$ denotes the 1st column of R. To include the vessel forward speed, $R_b^{hs}(\Theta_{hs-b})$ and $R_b^{hp}(\Theta_{hp-b})$, are approximated by eq.(8), but the resulting nonlinear couplings, are neglected [2]. Therefore, for sinusoidal motions, a linear approximation of equation (10) arises, from expanding the 6 DOF formulation of Perez [2], and is given by:

$$\dot{\boldsymbol{\xi}} = J_b^h \delta\boldsymbol{\nu} - \frac{U}{\omega_e^2} L \delta\dot{\boldsymbol{\nu}} \tag{12}$$

where $J_b^h = J_b^h(r^b_{\bar{o}hs}, r^b_{\bar{o}hp})$, $\delta\boldsymbol{\nu} = (\boldsymbol{\nu} - \bar{\nu})$ is the 9 DOF oscillating component of the velocity vector, in the b-frame, and $\bar{\nu} \approx [U, 0, 0, 0, 0, 0, U, 0, 0]^T$ is the 9 DOF surge velocity slowly-varying component linear approximation, expressed in the b-frame. ω_e is the wave encounter frequency, given in Perez [2], and the only non-zero elements of the L matrix are $L_{26} = L_{86} = 1$ and $L_{35} = L_{95} = -1$.

Given the accelerations in the b-frame, the accelerations in the h-space are:

$$\ddot{\boldsymbol{\xi}} = J_b^h \delta\dot{\boldsymbol{\nu}} + UL\delta\boldsymbol{\nu} \tag{13}$$

The transformation between the b and the n frame is non-linear and is given by:

$$J_b^n(\Theta_{n-b}) = \begin{bmatrix} R_b^n(\Theta_{n-b}) & 0_{(3\times 3)} & 0_{(3\times 3)} \\ 0_{(3\times 3)} & T_\Theta(\Theta_{n-b}) & 0_{(3\times 3)} \\ 0_{(3\times 3)} & 0_{(3\times 3)} & R_b^n(\Theta_{n-b}) \end{bmatrix} \tag{14}$$

The transformation between the b and the W frame is given by:

$$J_b^W(\Theta_{W-b}, r^b_{\bar{o}W}) = \hat{J}_b^W(\Theta_{W-b}) H(r^b_{\bar{o}W}, r^b_{\bar{o}W}) \tag{15}$$

where $\hat{J}_b^W(\Theta_{W-b})$ has the same form as eq.(14), and $H(r^b_{\bar{o}W}, r^b_{\bar{o}W})$ has the same form of eq.(9), and Θ_{W-b} are the Euler angles between the b and the W-frame, such that $\Theta_{W-b} = \Theta_{hp-b}$. The transformation between the b and the W-frame, given in eq.(15), is non-linear.

IV A 9 DOF Ship and Harvester Control Oriented Model

The 9 DOF dynamical model, shown in this section, includes the effects of forward speed, the wave and current loads, the ship propellers and motion control forces, and the winch motor dynamics.

This formulation arises by merging the unified ship model of Fossen [1], Perez [2] , including the seakeeping fluid memory effects, and the Nielsen [3], Fard [4] 9 DOF ship-crane coupled model, which includes an elastic coupling between the vessel and the payload, and computes the harvester hydrodynamic forces. For the ship-harvester elastic couplings, a stiffness matrix, based on Shashikala *et al* [6], has been computed. The motor dynamics are based on Messineo *et al* [7]. It's assumed that the motor is a three-phase AC servo motor, with an embedded speed regulator, such that the W-frame dynamics between the real motor speed, $v_m^W \equiv \dot{z}_m^W$, and the desired motor speed, v_d^W, is given by the first order system $\dot{v}_m^W = [-\lambda]v_m^W + [\lambda]v_d^W$.

As in the seakeeping theory, it's assumed that:

The sea is an ergodic stochastic Gaussian process, fully defined by its power spectrum, $S_{\zeta\zeta}(\omega_e, \chi)$.

Here, ω_e is the *encounter frequency* and χ is the vessel heading, as given in [2]. See [2], [9] for more details on seakeeping theory. For multidirectional sea waves, also called a short crested irregular sea [2], the spectral density is given by:

$$S_{\zeta\zeta}(\omega_e, \chi) = T_e(U, \chi)\big\{S(\omega)\big\}M(\bar{\chi}) \tag{16}$$

Where $M(\bar{\chi})$ is a directional spreading function, proportional to $\cos^{2n}(\bar{\chi})$, non-zero only for $-\pi/2 < \bar{\chi} < pi/2$, as in [2], where $\bar{\chi}$ is the vessel heading relative to the dominant wave heading, also called the *encounter angle*, and n is a *directional spreading factor*. In eq.(16), $S(\omega)$ is the spectrum for monodirectional sea waves, i.e a long crested sea [2]. A commonly used power spectral density function is the *JONSWAP* spectrum [1], [9], given by:

$$S(\omega) = 155\frac{H_s^2}{T_1^4}\omega^{-5}\ exp\left(\frac{-944}{T_1^4}\omega^{-4}\right)\gamma^Y \tag{17}$$

where H_s is the significant wave height, T_1 is the average wave period, given in [1], [2], γ is the spectrum peakedness factor, and Y is a function of ω and T_1, as given in [1]. In eq.(16), $T_e(U, \chi)$, is a doppler effect spectrum transformation, due to the vessel forward speed, given in [2]. The sea state realization is approximated by a finite Fourier series. The relationships between the power spectrum, $S_{\zeta\zeta}$, and the sea characteristics are given in [2] and [1].

The 9 DOF *ship slow manoeuvring and harvester altitude control oriented motion model*, in a seaway, with forward speed, in finite depth water, is therefore given by:

$$\begin{gathered}
\big[M_{RB}^b + M_A^b(\infty)\big]\dot{\boldsymbol{\nu}} = -(N^b(\infty) + D_r^b + C_{RB}^b)\delta\boldsymbol{\nu} \\
-D_v^b \cdot \delta\boldsymbol{\nu}|\delta\boldsymbol{\nu}| - C_r^b\mu - g^b(\boldsymbol{\eta}) - G_m^b(Z_m^W)\boldsymbol{\xi} \\
+\tau_w^b + \tau_p^b + \tau_c^b - M_m^b\lambda(V_d^W - \dot{Z}_m^W) + \tau_m^b(\dot{Z}_m^W), \\
\ddot{z}_m^W = \lambda(v_d^W - \dot{z}_m^W), \\
\dot{\mu} = A_r^b\mu + B_r^b\delta\boldsymbol{\nu}, \\
\dot{\boldsymbol{\eta}} = \ J_b^n(\Theta_{hb})\ \boldsymbol{\nu},
\end{gathered} \tag{18}$$

where:

$$M_{RB}^b = (J_b^h)^T M_{RB}^h J_b^h \tag{19}$$

is the rigid body mass, in the b-frame,

$$M_A^b(\infty) = (J_b^h)^T A^h(\infty) J_b^h \tag{20}$$

is the infinity frequency added mass matrix, in the b-frame,

$$C_{RB}^b = U M_{RB}^b L \tag{21}$$

is the centripetal and Coriolis matrix, in the b-frame,

$$N^b(\infty) = (J_b^h)^T[B^h(\infty) + U A^h(\infty)L]J_b^h \tag{22}$$

is the infinity freq. damping, including the forward speed effect, in the b-frame,

$$g(\boldsymbol{\eta})^b = (J_b^h)^T G\boldsymbol{\eta} \tag{23}$$

is the restoring force, in the b-frame. The only non-zero entries of the vectors Z_m^W, $\dot{Z}_m^W$, $\ddot{Z}_m^W$ and V_d^W are the 9th element, respectively z_m^W, $\dot{z}_m^W$, $\ddot{z}_m^W$ and v_d^W. $\tau_w^b = (J_b^h)\tau_w^h$ is the generalized first and second order wave force vector, in the b-frame, given in [2]. The first order wave forces arise from the linear potential theory [11], and are computed with the linear transfer function response amplitude operator *(RAO)* approach, see [2], [9] for more details. $\tau_p^b + \tau_c^b$ are the generalized propeller and ship motion control forces in the b-frame, given in [2] and [1]. $\tau_m^b(\dot{z}_m^W)$ is the motor generalized force vector in the steady state, which is a function of the motor speed $\dot{z}_m^W$.

The motor inertia matrix in the b-frame is given by:

$$M_m^b = (J_b^W)^T M_m^W \tag{24}$$

where J_b^W, is given in eq.(15). The only non-zero element of the motor mass matrix in the W-frame is $M_m^W(9,9) = m_m$, where m_m is the motor mass.

The inertial coupling between the ship and harvester are neglected in M^h_{RB} and $A^h(\infty)$, as in [4]. The ship (6×6) upper part of the matrices M^h_{RB} and $A^h(\infty)$ are in the same form as in [2], as for the upper part of $B^h(\infty)$, and $g(\boldsymbol{\eta})^b$. It's assumed that the harvester is a sphere, of radius r. The rigid body M^h_{RB} (3×3) lower matrix is $M^h_{RB_p} = Diag\Big\{m_l\Big\}$, where m_l is the payload mass. For the matrix $A^h(\infty)$, the (3×3) lower matrix is $A^h_p(\infty) = Diag\Big\{4/3\ \rho\pi r^3\Big\}$, where ρ is the water density, as given in [5], [9].

The radiation force fluid memory effects are computed only for the vessel, as shown in [2]. A simple linear diagonal damping matrix D_l is added to the (6×6) $B^h(\infty)$ matrix. A_r, B_r, C_r and D_r gives the fluid memory state space approximation of Cummins' equation [12], and are the same as in [2], computed only for the vessel 6 DOf, with the Kristiansen and Egaland [13] approach. The slow motor position component, $\bar{z}^W_m$, expressed in the W-frame, is assumed to approximate the cable nominal length, also referred as the *pendulum length*, l, when the cable is at rest, as in [7]. The total stiffness coupling matrix, $G^b_m(Z^W_m)$, in eq.(18), based on Shashikala *et al* [6], is given by:

$$G^b_m(Z^W_m) = \hat{T}^T\ K_c\ \widetilde{T}, \tag{25}$$

where $\hat{T} = H(r^b_{\bar{o}W}, r^b_{\bar{o}W})$, and $\widetilde{T} = H(r^{hs}_{\bar{o}W}, r^{hp}_{\bar{o}W})$, have the same for as eq.(9), and

$$K_c = \begin{bmatrix} K & 0_{(3\times3)} & -K \\ 0_{(3\times3)} & K & 0_{(3\times3)} \\ -K & 0_{(3\times3)} & K \end{bmatrix}. \tag{26}$$

In eq.(26), $K = Diag\{k_e\}$, where $k_e = AE/l_e$ is the rope stiffness, in which A is the cross-sectional cable area, E is the Young elasticity modulus, l is the pendulum length, and l_e is the effective cable length, including the elasticity effects. The point $r^b_{\bar{o}W}$, is the origin of the winch reference W-frame.

The hydrodynamic forces acting on the harvester are based on a modified Morrison equation [9], [5]. The hydrodynamic loads, acting on the harvester device, are:

$$\begin{aligned} \tilde{\tau}^h_{wp} = &+M^h_{RB_p}\tfrac{\mathrm{d}\bar{w}}{\mathrm{d}t} + \tau^h_s + \\ &B^h_p(\infty)(\bar{w} - \dot{\boldsymbol{\xi}}_p) + D^h_{v_p}(\bar{w} - \dot{\boldsymbol{\xi}}_p)|\bar{w} - \dot{\boldsymbol{\xi}}_p| \end{aligned}, \tag{27}$$

where the only non-zero element of τ^h_s is $\tau^h_s(3) = g(m_l - \rho\nabla)$, where $\nabla = 4/3\pi r^3$ is the displacement volume, $B^h_p(\infty) \approx Diag\Big\{\nabla\ C_{lv}\sqrt{r}g\Big\}$ is assumed to be the payload infinite frequency linear damping matrix [4], with $C_{lv} = 1$, and $D^h_{v_p} = Diag\Big\{\rho C_{dv} r^2\Big\}$ is the Morrison viscous drag [9], where the gain C_{dv} is approximated with the Clauss table, given in [9], for dominant inertia forces and low frequency waves, as $C_{dv} \approx 1.2$. The first term of equation (27) represent the Froude-Kryloff pressure forces, where the $\bar{w}$ is the fluid velocity vector, given by:

$$\bar{w} = \omega_e\zeta_a \begin{bmatrix} \Gamma_x(\boldsymbol{\eta})\cos(\chi)\sin(w_e - k\bar{x}) \\ -\Gamma_x(\boldsymbol{\eta})sin(\chi)\sin(w_e - k\bar{x}) \\ -\Gamma_z(\boldsymbol{\eta})\cos(w_e - k\bar{x}) \end{bmatrix}, \tag{28}$$

where ζ_a is the wave peak, $k\bar{x}$ is the wave space phase, $k = \omega^2_e/g$ is the wave number,

$$\bar{x} = \big(\boldsymbol{\eta}(7)\cos(\chi) - \boldsymbol{\eta}(8)\sin(\chi)\big) \tag{29}$$

as in [2], and

$$\Gamma_x(\boldsymbol{\eta}) = \tfrac{\cosh(k(h-\boldsymbol{\eta}(9))}{\sinh(kh)}, \quad \Gamma_z(\boldsymbol{\eta}) = \tfrac{\sinh(k(h-\boldsymbol{\eta}(9))}{\sinh(kh)} \tag{30}$$

come from the wave potential function, for a finite depth water, [9], [5]. The last term of eq.(27) is approximated by [9]:

$$D^h_{v_p}(\bar{w} - \dot{\boldsymbol{\xi}}_p)|\bar{w} - \dot{\boldsymbol{\xi}}_p| \approx D^h_{v_p}\Big(\bar{w}|\bar{w}| - \dot{\boldsymbol{\xi}}_p|\dot{\boldsymbol{\xi}}_p|\Big), \tag{31}$$

such that the functions of $\boldsymbol{\xi}_p$ can be moved to the left hand side, and the first term of eq.(31), is added to τ^h_w. The matrix D^b_v is obtained via eq.(19). Instead of the approximation of eq.(31), one can also use the *equivalent linearisation* method, shown in [9].

V Simulation Results

For the evaluation of different harvesting patterns, a simulator toolbox has been developed. The simulation environment is based on the open source Simulink MSS toolbox, developed by Fossen *et al* [8]. The sea state is simulated, for a short crested sea, using a JONSWAP spectrum, as in eq.(17), with $H_s = 3$ meters, $\gamma = 3.3$ [1], a cutoff frequency $f_c = 4.7143\ Hz$, 200 discrete uniform distributed random frequencies, 60 discrete directions, and a directional spreading factor of $n = 4$.

The vessel data are taken from the MSS example vessel $S175$ [14], computed using Seaway [15]. A vessel heading Nomoto PID controller [2], also included in the MSS toolbox, is used for course keeping. The harvester is assumed to be a sphere of aluminium, with radius $r = 0.5$ $[m]$, and mass $m_l = 1000$ $[kg]$. The thruster force is $\tau_p = 4.3067\ 10^6$ $[N]$, $Lpp = 175$ $[m]$ is the vessel length between perpendicularies [2], and $m = 24609$ is the vessel mass, in Tons. The winch is put on the stern of the vessel. The reference W-frame origin from the b-frame is $X_t = -(0.03 + 1)Lpp/2$, $Y_t = 0$, $Z_t = -3T$ and $T = 9.5$ $[m]$ is the ship draught. The ship length/breadth ratio is $L/B \approx 6.8898$.

In the example under analysis, the winch motor dynamic is neglected, and the cable is assumed to have a constant nominal length, $l = 5T = 47.5$ $[m]$. The average altitude of the harvester, the z component of the $r^b_{\bar{o}hp}$ is $l - Z_t \approx 19$ $[m]$. The cable elasticity stress is $AE = 3.96\ 10^9$ $[N]$. The water depth is $28T = 266$ $[m]$. The vessel average forward speed is $U = 4.4$ $[m/s]$. Figure 3 shows the the harvester heave RMSE and variance, as a function of $\bar{\chi}$. The threshold for the solution optimality is 0.6 $[m]$. The optimal pattern heading, which reduces the harvester heave disturbance RMSE and variance, under the given threshold, lies between $[-40\ ,\ 40]$ degrees.

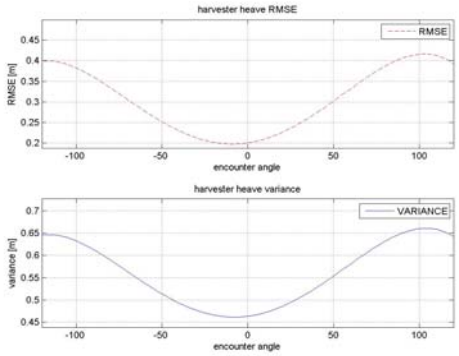

Fig. 3: *Harvester heave RMSE and variance, for different encounter angles,* $\bar{\chi}$

VI Conclusions

In this paper, a 9 DOF seaweed harvester model and a simulation toolbox are presented. Then, an optimal harvesting path orientation, which minimizes the wave induced harvester motion, is evaluated, by simulating several pattern headings, for a particular vessel, harvester and sea state. Several winch positions on the vessel can be chosen, for design purpose. The hydrodynamic vessel and harvester data can by obtained by using standard seakeeping softwares, such as Seaway [15], Veres [16] and Wamit [17]. The 9 DOF model, presented in this paper, can be used for the vessel and harvester motion control design, and validation.

References

[1] T. Fossen, *Marine Control Systems: Guidance, Navigation and Control of Ships, Rigs and Underwater Vehicles*, M. Cybernetics, Ed., Trondheim, 2002.

[2] T. Perez, *Ship motion control. Course keeping and roll stabilization using rudder and fins.* Springer, 2005.

[3] F. Nielsen, *Lecture Notes in Marine Operations*, Norwegian University of Science and Technology Std., 2007.

[4] M. Fard, "Simulation of coupled vessel-load dynamics," E&P Load and Responses R&T, Bergen, Tech. Rep., 2001.

[5] O. Faltinsen, *Sea Loads on Ships and Offshore Structures.* Cambrige University Press, 1990.

[6] A. Shashikala, R. Sundaravadivelu, and C. Ganapathy, "Dynamics of a moored barge under regural and random waves," *Ocean Engineering*, vol. 24, no. 5, p. 401:430, 1997.

[7] S. Messineo, F. Celani, and O. Egeland, "Crane feedback control in offshore moonpool operations," *Control Engineering Practice*, vol. 16, p. 356:364, 2008.

[8] T. Perez, O. Smogeli, T. Fossen, and A. Sorensen, "An overview of the marine system simulator MSS: A Simulink toolbox for marine control systems," *Modelling, Identification and Control*, vol. 27, no. 4, p. 259:275, 2006.

[9] J. M. Journee and W. W. Massie, *Offshore Hydromechanics - First Edition*, D. U. of Technology., Ed., 2001.

[10] T. Perez and T. Fossen, "Kinematic models for seakeeping and manoeuvring of marine vessels," *Modeling, Identification and Control*, vol. 28, no. 1, p. 1:12, 2007.

[11] F. Ursell, "On the heaving motion of a circular cylinder on the surface of a fluid," *Quarterly Journal of Mechanics and Applied Mathematics*, vol. 2, p. 218:231, 1949.

[12] W. Cummins, "The impulse responce function and ship motion," David Taylor Model Basin-DTNSRDC, Tech. Rep. 1661, 1962.

[13] E. Kristiansen and O. Egeland, "Frequency dependent added mass in models for controller design for wave motion ship damping," in *6th IFAC Conference on Manoeuvring and Control of Marine Craft MCMC'03*, Girona, Spain, 2003.

[14] T. Fossen, *Description of MSS Vessel Models: Configuration Guidelines for Hydrodynamic Codes*, June 2008.

[15] *SEAWAY for Windows Product Sheet*, Delft University of Technology, Amarcon BV, 2009.

[16] Marintek, *Integrated Ship Design Tool Hydrodynamic Workbench ShipX.*

[17] *WAMIT User Manual, Version 6.4, 6.4PC, 6.4S, 6.4S-PC*, Wamit inc., available online on www.wamit.com.